DIRECT DRIVE SYSTEMS WITH TRANSVERSE FLUX RELUCTANCE MOTORS

Ioan-Adrian VIOREL[*], Mircea CRIVII[**], Lars LÖWENSTEIN[***], Loránd SZABÓ[*], Mircea GUTMAN[*]

*Technical University of Cluj, Electrical Machines Department, 15 C. Daicoviciu str., 400020 Cluj, Romania, e-mail: ioan.adrian.viorel@mae.utcluj.ro,
** EPFL, LAI, Ecublens CH 1015 Lausanne, Switzerland, e-mail: mircea.crivii@epfl.ch
***SIEMENS Transportation Systems, Erlangen, Germany, e-mail: lars@loewenstein.info

Abstract – The transverse flux motor (TFM), quite a new concept of an electric machine, begins its impetus in the late 80s of the last century. The transverse flux reluctance motor (TFRM) is a variant of TFM with passive rotor and simpler construction. The achievable power TFRMs' to total machine weight ratio is smaller than for TFM with permanent magnets on the rotor (PMTFM), but larger than for conventional machines. Since TFRM has a large number of poles the motor is well suited for variable low speed direct drive applications. TFRM actual state-of-art will be presented in the paper with more strength on its construction, design, supply control and applications. Partly being a review of the already published information the paper contains some original developments concerning mainly TFRM design.

1. Introduction

The transverse flux (TF) machine looks like a newcomer in the electrical machines family, but it has quite a long history. In fact the claw-pole flux pattern implies the transverse flux concept and the claw-pole alternator is the oldest three phase electric machine. In 1885 W.M. Morday applied for a patent concerning the transverse flux machine, but the machine was named, and brought back to the scene by Weh in the 80s [1, 2]. Weh introduced first the TF machine's very dedicated topology, which usually includes the flux concentration principle for the permanent magnets excited structures. Since the TF machine allows the pole number to be increased without reducing the MMF per pole, it is capable of producing power densities much greater than a conventional machine.

The achievable power to total machine weight ratios for active rotor TF machines ranges between 0.5-2 kW/kg compared to 0.25-0.8 kW/kg for conventional machines [3, 4, 5].

Due to this very large value of power to total weight ratio the TF machine looks very attractive to some specific drives where the electric machine weight limitation is one of the most important requirements.

The TFR machine is a variant of the TF machine with passive rotor. It has a ring winding with salient poles on the stator, and only salient poles on the rotor. It behaves like a switched reluctance (SR) machine, the main difference consisting on the homopolar stator winding. Each phase of the TFRM is an independent module, as shown in Figs. 1 and 2. The TFRM must have three or more than three phases in order to avoid the start-up difficulties and to obtain continuous rotation [6, 7].

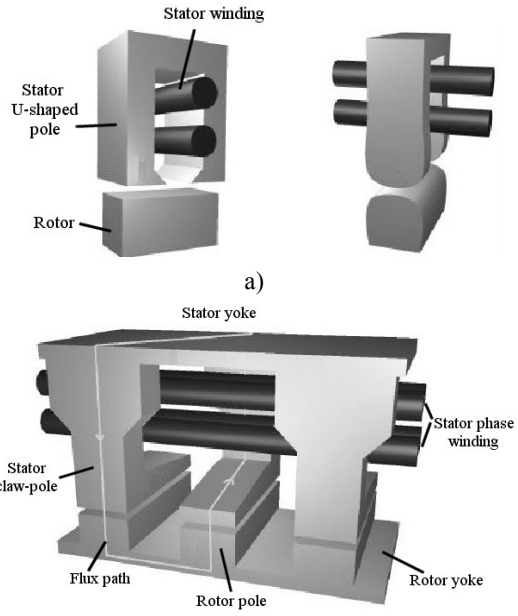

Fig. 1. Basic structure of a TFR machine: a) with U-shaped poles, b) with claw-poles [6]

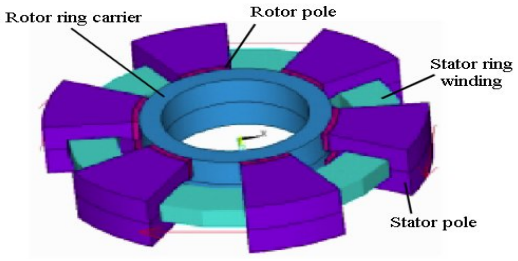

Fig. 2. Six pole TF reluctance machine, one phase, poles in aligned position [4]

The TFRM is supplied via an asymmetric half bridge electronic converter, each phase being independent. The converter gives unipolar pulses synchronized with the rotor position.

Some TFRM specific constructions and proposals on motor's design or sizing are given in [6, 7, 8, 9, 10, 11], but not only. A 3D to 2D equivalence which allows for using only 2D FEM analysis instead of a 3D-FEM analysis to calculate the

motor's characteristics and performance is presented in [7, 12]. Other references deal with TFRM mathematical models [6, 7, 10, 13, 14, 15, 16], or with specific applications as crankshaft starter-alternator [6, 13, 15].
In this paper the most important aspects concerning TFRM are covered, with more strength on its construction, design, supply, control and applications. The paper contains some original developments, mainly on TFRM design, scaling and models, not only a review of the already published information.

2. TFRM construction and design

The TFRM has, for each phase, a toroidal winding which is placed on the stator. Usually such a motor has no permanent magnets (PMs), but there were proposed some variants also with PMs which help the excitation, [8] for instance. The TFRM stator iron core has two basic structures:

i) With U-shape poles which have both teeth in the same axial plane, Fig 1a.
ii) With claw-poles shifted between them, Fig 1b.

The TFRM with U-shapes poles, Fig 1a, has only a 2D flux pattern, the transverse flux being almost nil. TFRM with claw-poles, Fig. 1b, has a true 3D flux pattern, where the transverse flux is important. In both cases the torque is of reluctance type and the passive rotor has salient poles as in the switched reluctance motor (SRM) case.
The TFRM has the simplest topology of all TFMs. It has quite the same features as the SRM, the main differences being:

i) TFRM has homopolar type stator phase winding.
ii) Each phase is an independent module, Fig. 2.
iii) TFRM's phase modules are placed consecutively in the axial direction.
iv) TFRM has the same number of poles on the stator and on the rotor.

In order to avoid start-up difficulties and to obtain continuous rotation TFRM must have minimum three phases. The TFRM phases work independently hence the increasing of the number of phases does not lead to a proportional power output increase, but reduces the torque ripples. The TFRM has to be supplied trough a power electronic converter which generates unipolar phase currents precisely synchronized with the rotor position. The electronic converters are quite of the same type as that used to supply SRMs.
TFRM design procedure is not that simple and employs usually four steps:

i) A sizing-estimation procedure which offers a first design data for the machine starting from the design requirements.
ii) A 2D- or 3D-FEM magneto-static and quasitransient analysis, which offers the possibility to optimize the motor's magnetic circuit and to compute the iron core losses and the motor characteristics.
iii) A thermal analysis done by using a thermal equivalent circuit [3] or a 2D-FEM analysis of the thermal field through the motor.
iv) A drive system computer simulation to study the dynamic behaviour of the motor, when it is supplied by a specific electronic converter and it is fully controlled function of the imposed drive requirements.

In this chapter the first two steps concerning the TFRM's design procedure will be briefly discussed. The thermal analysis does not imply some specific aspects since the TFRM structure is very simple, (it has no PM's and the winding is only on the stator). The TFRM dynamic behaviour will be covered in the following chapter, when the supply and control strategy will be presented, too.
The TFRM sizing equation is obtained from output power, which is:

$$P_{out} = \eta \frac{E_{\max}}{K_E} \frac{I_{\max}}{K_I} \tag{1}$$

where E_{max} and I_{max} are the maximum values of the armature winding EMF and current, K_I, K_E are waveform factors [4, 11] and η is the efficiency.
The air-gap reluctance varies, as in the SRM's case, and the air-gap flux density variation between unaligned and aligned rotor position can be approximated by:

$$\Delta B_g = 2B_{g\max}\left(1 - \frac{1}{K_{CR}}\right) \tag{2}$$

B_{gmax} being the aligned air-gap flux density and k_{CR} the Carter's factor, computed by considering saliency only on the rotor [3, 4].
If the stator electrical loading A_s is

$$A_s = \frac{N_t I_{\max}}{\pi D_g} \tag{3}$$

N_t and D_g being the phase number of turns and respectively the air-gap average diameter, then

$$P_{out} = K_M D_g^3 B_{g\max} A_S Q_R n \tag{4}$$

where Q_R and n are the rotor number of poles, respectively speed.
The specific motor coefficient is:

$$K_M = 2\pi^2 \eta k_p k_{ov} k_L (1 - 1/k_{CR})/k_E \tag{5}$$

k_p and k_{ov} being two sizing factors [3, 4, 8, 9], while the aspect ratio factor k_L is:

$$k_L = l_R / D_g \tag{6}$$

where l_R is the axial length of one phase module.
Once the designer has chosen the number of poles Q_R, the specific values for aligned air-gap flux density B_{gmax} and for stator electrical loading A_s, as for the sizing factors, Carter's factor and aspect ratio, and has the required design data, output power and speed, efficiency and power factor he can calculate the average air-gap diameter and all the stator and rotor main dimensions [4, 11].
The average torque per phase T is [4]:

$$T = \frac{1}{2} Q_R N_t I A_p \frac{B_{g\max}}{\Delta\theta} \tag{7}$$

where A_p is the stator pole area and $\Delta\theta$ is the rotor angular displacement between an aligned and an unaligned position.
The power can be computed, and the iron and winding losses, too, as for conventional machines [4, 11].
The scaling procedure is a very helpful tool in obtaining fast design draft for a TFM, if the data of similar motor are available. Scaling, a particular case of a general similitude transformation, leads, under imposed constraints to a fully similar model of an original TFRM. If the specific motor coefficient is kept constant (5), then adequate conditions can be imposed in order to obtain a fully scaled model starting from an originally given motor.
The restrictions required are concerning the way the magnetic field quantities are scaled, which means that, if k_{sc} is the length scaling factor then the magnetic flux density B is kept constant, while the magnetic vector potential has to be scaled by the length factor k_{sc} and the current density by its inverse. With the same material the reluctivity remains invariant. Since the flux density is constant, the MMF produced by the exiting coil must be scaled by length scaling factor k_{sc} while the coil number of turns is invariant in the scaling process.
In Table 1 the main data and the analytically calculated outputs of an original and scaled TFRM are given, the scaling factor being $k_{sc} = 0.5$.

	Symbol	Unit	Original	Scaled
Air-gap diameter	D_g	mm	100	50
Stator pole width	b_{Sp}	mm	26	13
Air-gap length	g	mm	0.3	0.15
Pole axial length	l_{Sp}	mm	14	7
Phase MMF	F	A	463	231.5
Maximum air-gap flux density	Bg	T	0.969	0.969
Maximum torque per phase	T	Nm	0.936	0.117

Table 1 Main data and output for original and scaled TFRM

The variation of the static torque for the original and scaled TFRM versus rotor displacement, calculated via a 3D-FEM analysis, are given in Fig. 3, the values being in good agreement with the analytically computed ones, Table 1.

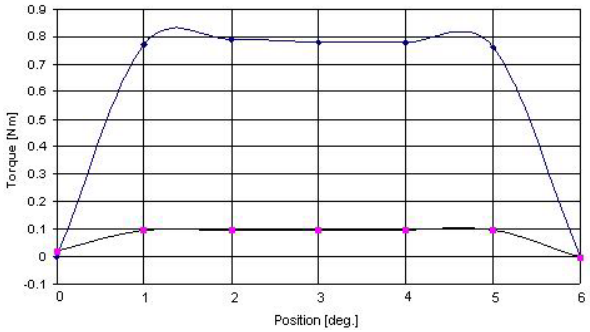

Fig. 3. Static torque versus rotor position

The concordance between the 3D-FEM and respectively calculated values are fairly good and in the case of the air-gap flux density of both, original and scaled, motors. The axial variation of the air-gap flux density is given in Figs. 4 and 5 for the original and respectively scaled TFRM, in aligned position.

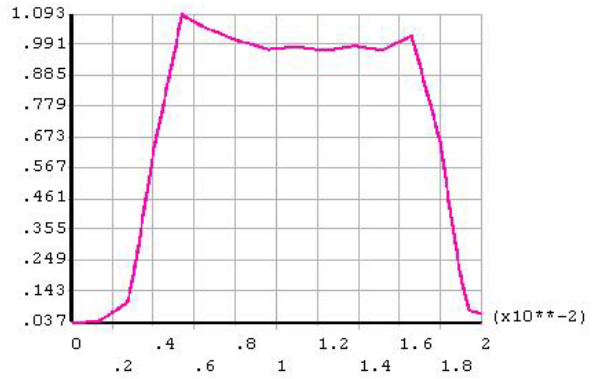

Fig. 4. Air-gap flux density axial variation, original TFRM, aligned position

Fig. 5. Air-gap flux density axial variation, scaled TFRM, aligned position

Since an important step in the designing procedure of a TFRM consist in 2D- or 3D-FEM analysis an equivalence defined between 3D and 2D models [12] is of quite great importance. As shown in [12] there is a possibility to define an equivalent SRM to the analyzed TFRM and to apply a 2D-FEM on this model in order to calculate the TFRM characteristics. The imposed conditions for the equivalent SRM are [12]:

i) The same number of poles.
ii) The same average air-gap diameter and pole width.
iii) A double air-gap length.
iv) The pole MMF equal with the TFRM phase MMF.

Considering this equivalence the SRM model of the original TFRM whose data are given in Table 1 has the aligned air-gap flux density B_{gmax}=0.878 T compared with 0.936 T for the TFRM (3D-FEM). The torque is 0.936 Nm for TFRM (3D-FEM) and 0.822 Nm for equivalent SRM, values which show a very good concordance.
Taking into account this 3D to 2D equivalence the TFRM magnetic field can be analyzed by using two 2D-FEM

models, one axially defined in aligned position and one circumferentially for the equivalent SRM.

3. TFRM supply and dynamics

The TFRM supply is assured through an electronic converter which is quite the same as the one used in the SRM's case. The most usual converter, an asymmetric bridge for a three phase TFRM, which has the phases completely independent, is shown in Fig. 6.

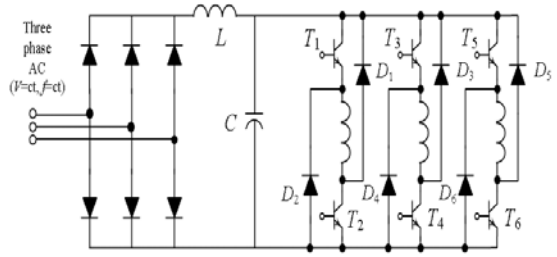

Fig. 6. Three-phase TFRM's electronic converter.

There are two control strategies, but in both cases the current is controlled in a PWM mode. In the first case the transistors in series with one of the TFRM's phase, T_1 and T_2 for example, Fig. 6, are turned *on* and *off* simultaneously. In the second case T_1 is turned *on* for the entire phase duty cycle and the phase current PWM control is done by turning *on* and *off* T_2. In the first case when T_1 and T_2 are turned *off* the energy stored in the phase is sent to the source resulting repeatedly energy exchange between the load and the source in one duty cycle.

The second control strategy is different since there is no energy exchange between the source and the load during the duty cycle, but at its end when T_1 and T_2 are turned *off* simultaneously. This control strategy assures a self circulation of the energy and consequently, since the current is kept going on for longer time, results a longer current tail than in the first case when the source is recharged and the current can be turned *off* rapidly. It is obvious that the first control strategy is more adequate in the TFRM's case, even it causes many ripples into the DC link capacitor, Fig. 6, and an increase in the switching losses of the power electronic device.

Both control strategies can be implemented by using for the current control a hysteresis type controller which computes the current error, compare it with the imposed value error, and gives adequate command signals on the transistor's gate.

The TFR machine is capable of operating continuously as a generator supplied by an electronic converter of the type presented in Fig. 6, since it can provide reverse voltage to the phase winding through freewheeling diodes. The TFR machine becomes generator after the aligned position, when the phase inductance decreases. The excitations power must be first supplied from the source and generating power is obtained during the de-fluxing period. It is possible to separate the excitation circuit from the output circuit by means of the circuit of the boost (up) converter Fig.7a, or of the buck (down) converter, Fig. 7b.

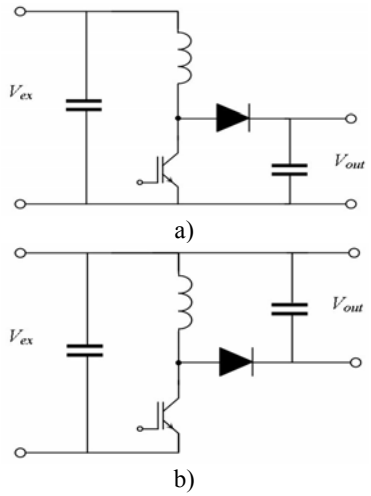

Fig. 7. TFR generator circuit based on a) boost and b) buck type converter.

The buck type converter, Fig. 7.b, seems to show up better performance since at a given speed the generating cycle is extended approximately in the ratio of the input to output voltage compared with the excitations period and consequently a larger generated energy can be obtained for the same input power.

Since the TFRM behaves almost as the SRM its control is quite similar. The TFRM requires rotor positioning sensing in order to commutate the current from phase to phase synchronously with the rotor position. An encoder or resolver attached to the TFRM's shaft is the usual solution for detecting the rotor position, but it can be applied also one of the developed methods for the indirect sensing of the rotor position. In Fig. 8 the basic control block diagram of the TFRM control system is shown. The system consists of a speed controller, a current controller if necessary, a firing angle control block and an encoder. The usual control strategy is a current control one.

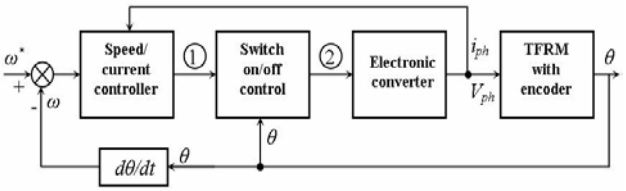

Fig. 8. TFRM drive control system, block diagram.

A good drive system cannot be obtained only with very well designed and constructed motors. It requires a suitable power electronic converter and adequate torque, speed and current controllers. Computer simulation of the entire drive system enables verification of the motor design and of the drive system ability to match the load torque over the entire speed range in steady-state and transient regime. The steady-state regime can be covered adequately with the simplified mathematical model used for design-estimation, or by finite element (FEM) analysis [4]. Simulation of the entire drive system requires the mathematical model of the TFRM and of the other components as well as their interconnections.

The TFRM has independent phases, then its mathematical model is given by the phase equations:

$$v = R \cdot i + \frac{d\lambda}{dt} \tag{8}$$

$$\lambda = L(\theta, i) \cdot i \tag{9}$$

$$T = \frac{\partial W_m}{\partial \theta} = \frac{d}{d\theta} \int_0^i \frac{1}{2} \lambda(\theta, i) \cdot di \tag{10}$$

$$T = J \frac{d\Omega}{dt} + T_f + T_l \tag{11}$$

where v, i, λ and R are the phase voltage, current, flux linkages and resistance and T, T_l, T_f, are the electromagnetic, load and friction torque respectively.

The rotor position electric angle θ is given by the equation:

$$\frac{d\theta}{dt} = \omega = p \cdot \Omega \tag{12}$$

where the number of pole pairs p is equal to the number of stator, or rotor, pole pieces, Q_S=Q_R.

The friction torque depends on the machine speed, but usually it has smaller value and can be neglected against the load torque at low speed.

The TFRM design procedure implies, quite usually, a FEM analysis and consequently the variation of the phase flux linkages and torque function of the rotor angular position and phase current are known. These can be used in computing the steady-state or dynamic characteristics of the TFRM.

Based on the given mathematical model (8)÷(12) and on the flux linkages and torque characteristics computed, via a 3D or 2D FEM analysis, function of phase current and rotor angular position in [7] and [13] the TFRM dynamic regime was simulated via SIMULINK and SIMPLORER respectively. In the SIMULINK program the characteristics obtained by FEM computation were introduced as look-up tables. The SIMPLORER program was linked to the FLUX 3D FEM software and the computation was done in the same time in both programming environments.

In Fig. 9 the results of a TFRM start-up dynamic regime simulation are given [4, 6]. Its starting required torque is 200 Nm and after the run-up the load torque is reduced to represent the considered loading machine, the application is an integrated starter-generator.

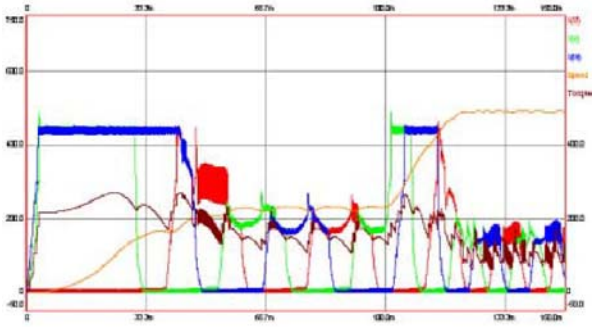

Fig. 9. TFRM dynamic regime at starting

In the case of the TFRM a simplified mathematical model, which does not require FEM analysis, but can be used to study the dynamic regime, briefly presented in following. The model is based on an air-gap variable equivalent permeance, which is defined as:

$$P(\theta, i) = \frac{1}{g^*}(1 + P_R \sin\theta) \tag{13}$$

where P_R is the permeance coefficient calculated considering saliency only on the rotor, [4], and g^* is the equivalent air-gap.

$$g^* = k_{CR} \cdot k_s \cdot g \tag{14}$$

Carter's factor k_{CR} is calculated with saliency on the rotor [4] and the saturation factor k_s depends on the phase current and can be computed in aligned position with or without FEM analysis.

The variable air-gap flux density is:

$$\begin{aligned} B_g(\theta, i) &= F \cdot \mu_0 \cdot P(\theta) \\ B_g(\theta, i) &= F \cdot \mu_0 \cdot \frac{1}{g^*}(1 + P_R \sin\theta) \end{aligned} \tag{15}$$

where F is the phase MMF.

The maximum value of the air-gap flux density occurs at aligned position,

$$B_{g\max}(i) = B_g(\theta, i)_{\theta=\pi/2} = F \cdot \mu_0 \frac{1}{g^*}(1 + P_R) \tag{16}$$

and consequently:

$$B_g(\theta, i) = B_{g\max}(i) \frac{1 + P_R \sin\theta}{1 + P_R} \tag{27}$$

The phase inductance is:

$$L(\theta, i) = \frac{\lambda(\theta)}{I} + L_{S\sigma} \tag{18}$$

where $L_{S\sigma}$ is the phase leakage inductance, which is considered constant.

Finally comes:

$$L(\theta, i) = M_d(i) \frac{1 + P_R \sin\theta}{1 + P_R} + L_{S\sigma} \tag{39}$$

with the aligned inductance M_d,

$$M_d(i) = \frac{B_{g\max}(i) \cdot N \cdot A_p \cdot Q_S}{I} \tag{20}$$

N, A_p and I being the phase number of turns, the stator pole area and the phase current.

By now the flux linkages derivative and the torque are:

$$\frac{d\lambda(\theta, i)}{dt} = \left(M_d(i) \frac{1 + P_R \sin\theta}{1 + P_R} + L_{S\sigma} \right) \frac{di}{dt} + \omega M_d(i) \frac{P_R \cos\theta}{1 + P_R} \cdot i \tag{41}$$

$$T = \frac{\partial W_m}{\partial \theta} = k_T \cdot i \cdot \cos\theta \tag{22}$$

with

$$k_T = \frac{N}{2} \cdot Q_S^2 \cdot A_p \cdot \frac{P_R \cdot B_{g\max}}{1 + P_R} \quad (5)$$

Based on a SIMULINK developed program the phase voltage, current and torque variation, for only one phase duty cycle, are shown in Fig. 10, 11 and 12 for a TFRM with the following main data:

i) Rated power P_{out} = 24 kW.
ii) Rated phase voltage V_{ph} = 300 V.
iii) Rated phase current I_{ph} = 150 A.
iv) Maximum phase current I_{phM} = 200 A.

The control strategy is one which allows turning *off* both transistors in series per phase, the initial position being considered unaligned one θ=0, and the aligned position for the considered phase is the final one.

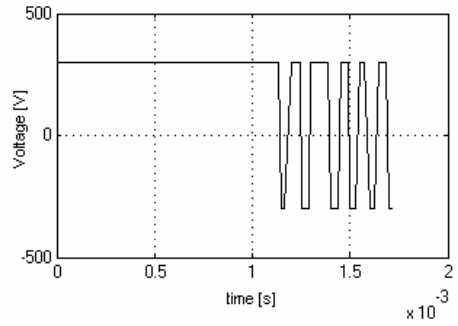

Fig. 10. Phase voltage versus time.

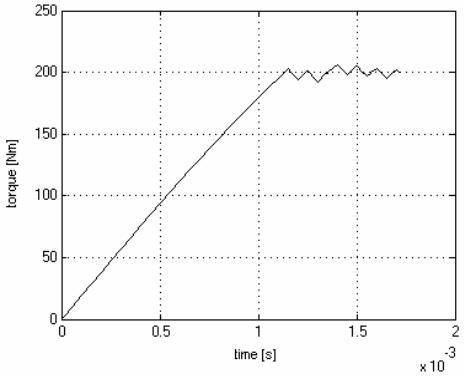

Fig. 11. Phase current versus time.

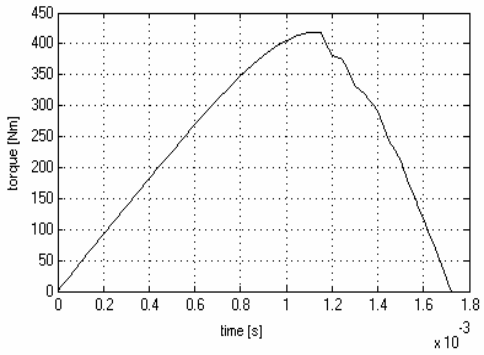

Fig. 12. The variation of torque versus time, for TFRM during a run-up regime for one stroke

The obtained characteristics, Fig. 10, 11 and 12 are quite the usual one, the current and torque increasing slope being limited by the phase inductance which is quite important for such a motor.

4. TFRM applications. Trends

A possible application of TFRM is a direct drive system for an electric vehicle (EV) or a hybrid electric vehicle (HEV). Such an application was considered and three type of motors were special designed for this purpose, a PMTFM, a SRM and a TFRM. The design specification were the output power, P_{out} = 25 kW and the rated speed n=600 rpm.

The PMTFM and TFRM have exterior rotor, a favourable solution for the first one which has PM's on the rotor, but adopted for the second in order to have the same stator dimensions.

The average air-gap diameter is D_g = 0,295 m and the air-gap length is g = 0.8 mm. The PMTFM is single sided with flux concentrating rotor topology and was the one designed, constructed and tested [4]. The main data are given in Table 2.

Feature	**Units**	**TFM**	**SRM**	**TFRM**
Stator/rotor pole number	-	80/80	6/4	50/50
Stator phase current	A	60	105	67.5
Efficiency	-	0.940	0.943	0.968
Inverter power	kVA	37.51	38.99	40.35
Specific torque T_{out}/G	Nm/kg	62.2	4.8	21.38
Torque per motor volume T_{out}/V	Nm/dm^3	58.3	7.19	20.7
Specific power P_{out}/G	kW/kg	1.30	0.1	0.45

Table 2 Motors' comparison for a direct drive

The results show that at this low speed the SRM with low number of pole, 6/4, is not a real competitor and that PMTFM has better performance compared with TFRM except the cost and the construction complexity.

A TFRM was proposed as a crankshaft starter-generator [4, 6, 13], its main data being:

i) Starting required torque: 200 Nm
ii) Overall axial length: 80 mm
iii) Exterior and air-gap diameter 320/200 mm
iv) Rated phase voltage: 42 V.

The designed TFRM has a particular topology of the stator poles and in order to reduce the leakage flux in the unaligned position the stator tooth tip width was skewed by 15% [6]. The counter part application was considered a 16/12 SRM

which had smaller time constant. In Fig. 13 the laboratory prototype converter is presented. In Fig. 14 a car engine equipped with a crankshaft started-alternator is given.
There are some possible applications which were not, to the author's knowledge, proposed and analyzed until now. Since TFRM has a quite good output power to weight ratio and a large starting torque it can operate as actuator for special purposes, i.e. heavy duty robotics, and not only.

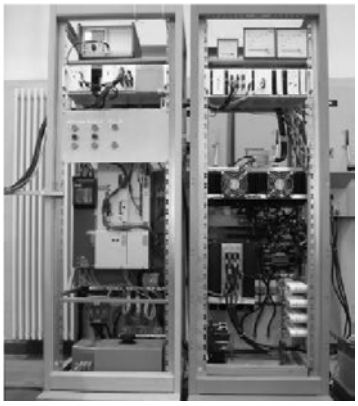

a)

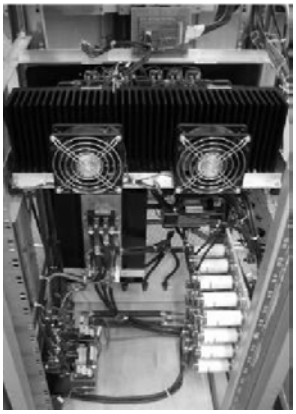

b)

Fig. 13. Prototype converter for TFRM a) general view, b) detail

Fig. 14. Car engine equipped with a crankshaft starter-alternator

The studies carried out until now, as well as the results obtained with already constructed prototypes, reveal a great future potential for TFRM applications. They show also a steadily improvement of the TFRM drive performance due to new topologies, materials and control strategies.

Acknowledgements

The work was possible due to the support given by the Romanian Academy under grant 106/2003 and was carried out in co-operation with the Dept. of Electrical Machines of RTWH Aachen, Germany. The researches were supported also by the Romanian National Council of Scientific Research in Higher Education through a grant offered.

References

[1] Weh, H. and Jiang, J., "Berechnungsgrundlagen fur Transvesalflussmaschinen", *Archiv f. Elektrotechnik*, vol. 71, 1988, pp. 187-198.

[2] Weh, H., Hoffmann, H. and Landrath, J., "New permanent magnet excited synchronous machine with high efficiency at low speeds", *Proc. of ICEM'88*, Pisa, Italy, pp. 1107-1111, 1988.

[3] Henneberger, G. and Viorel, I.A., "*Variable reluctance electrical machines*", Shaker Verlag, Aachen, Germany, 2001.

[4] Viorel, I.A., Henneberger, G., Blissenbach, R. and Löwenstein L., "*Transverse flux machines. Their behaviour, design, control and applications*", Mediamira Publishing Company, Cluj, Romania, 2003.

[5] Viorel, I.A., Hennenberger, G., and Blissenbach, R., "Rotating transverse flux machine, a review" *Proc. of Conference "Romanian Academy Days in Timisoara",* Romania, 2003, on CD.

[6] Lowenstein, L., "*Kurbelwellen-Starter-Generatoren auf der Basis von Reluktanz maschinen*" Ph.D. Thesis, RWTH Aachen, Germany, 2003.

[7] Kruse, R., Pfaff, G., Pfeiffer, C., Wehner, H.I., and Hopper, E., "New concept of a low-speed direct servodrive", *Proc. of PCIM '98, vol. Intelligent Motion*, pp. 1-10, 1998.

[8] Viorel, I.A., Popan, A.D., Blissenbach, R. and Henneberger, G., "On a transverse flux motor with permanent magnets in the stator", *Electromotion*, vol. 10, no. 4, pp. 420-425, 2003.

[9] Blissenbach, R., Henneberger, G. and Viorel, I.A., "On the single-sided transverse flux machine design," *Electric Power Components and Systems*, vol. 31, no.2, pp.109-128, 2003.

[10] Kruse, R., "Calculation methods for a transverse flux reluctance motor", *Proc. of. OPTIM*, 2000 Brasov, Romania, pp. 387-392.

[11] Viorel, I.A., Popan, A.D. and Barz, V., "On the single-sided transverse flux reluctance machine design" *Oradea University Annals*, Romania, 2003, vol. 13, pp. 348-354.

[12] Crivii, M., Viorel, I.A., Jufer, M. and Husain, I., "3D to 2D equivalence for a Transverse Flux Reluctance Motor", *Proceedings of ICEM '02*, Brugge, Belgium, on CD-ROM, 2002.

[13] Lowenstein, L. and Henneberger, G., "Development of a Transverse Flux Reluctance Machine for a crankshaft starter-alternator", *Proc. of SPEEDMAN'00*, pp. BB1.19-BB1.22, Ischia, Italy, 2000.

[14] Viorel, I.A., Blissenbach, R., Henneberger, G. and Popan, A.D., "The transverse flux motor mathematical model", *Revue Roumaine des Sciences Techniques – Série Electrotechnique et Énergétique.,* vol. 48, no. 2/3, pp 369-379, Bucharest, 2003.

[15] Zacharias, L., Lowenstein, L. and Hennenberger, G., "Crank shaft starter generators based on the principle of reluctance" *AutoTechnology*, no. 6, pp. 68-71, Vienweg Verlag, Wiesbaden, Germany, 2002.

[16] Viorel, I.A., Szabo, L. and Şteţ, C., "Dynamic regime of the transverse flux reluctance motor" *Proc. of Conf.* "Romanian Academy Days in Timişoara", Romania 2003, on CD-ROM.

[17] Löwenstein, L.,and Henneberger, G., "Dynamic simulation of a crankshaft starter alternator", *Proceedings of the GPC – Global Powertrain Congress, vol. Advanced Propulsion and Emission Technology*, pp. 141-146, Detroit, USA, 2001.

[18] Blissenbach, R., and Henneberger, G., "Numerical calculation of 3D eddy current fields in transverse flux machines with time stepping procedures", *The International Journal for Computation and Mathematics in Electrical and Electronic Engineering (COMPLE)*, vol. 20, no.1, pp.152-166, 2001.

[19] Muljadi, E., Butterfield, C.P., and Wan, Vin-Huie, "Axial-flux modular permanent-magnet generator with a toroidal winding for wind-turbine application", IEEE *Trans. on IA*, vol. 35, no. 4, 1999, pp. 831-836.

[20] Masmoudi, A., and Elantably, A., "Cogging torque reduction in TFPM machines: Comparison between two alternatives", *Proc. of ICEM '02*, Brugge, Belgium, on CD-ROM.